Australian Earthquake Engineering Society
2024 National Conference, 21-23 November 2024
Adelaide, South Australia

Neotectonic Features in the Snowy Monaro Region, NSW

Bethany Eaton[1], Jonathan Griffin[2], Mark Quigley[1], Dan Clark[2], Tamarah King[2]

Contact: Bethany Eaton - bleaton@student.unimelb.edu.au

1. School of Geography, Earth, and Atmospheric Science at the University of Melbourne, 253-283 Elgin St, Carlton VIC 3053

2. Community Safety Branch, Geoscience Australia, 101 Jerrabomberra Ave, Symonston ACT 2609

Abstract

The Snowy Monaro region of NSW hosts infrastructure critical to Australia's water and energy security. The region also contains several neotectonic features that show evidence for earthquake activity since the current crustal stress regime has been in place, and therefore has the potential to produce large future earthquakes. Here, we present detailed structural and geomorphic evidence from 2 m resolution lidar digital elevation models, geological maps and geophysical data for surface-rupturing neotectonic features in the region. We improve the accuracy and mapping precision of known features and identify evidence for five previously unmapped features. Evidence is characterised using confidence classifications and a Geomorphic Indicator Ranking (GIR) system and each neotectonic feature is assigned a confidence level ranging from *A* (Definite neotectonic feature) to *D* (Unlikely to be a neotectonic feature). Maximum moment magnitude ($M_{w,max}$) estimates for single-fault rupture scenarios are presented. Our data will inform national-scale and site-specific seismic hazard analyses.

Keywords: Neotectonics; NSW; Snowy Mountains; Remote mapping; Surface ruptures

1 Introduction

Large earthquakes may leave signatures in the landscape which, if preserved, can be used to identify active faults that may be expected to host future earthquakes. A key component of a seismic hazard assessment is the identification and characterisation of fault traces which represent ground surface rupture. The dimensions of mapped fault traces can be used with source-scaling regressions to estimate maximum earthquake magnitudes (Leonard, 2014; Wells & Coppersmith, 1994; Yang et al., 2021). The age of geomorphic features displaced by faults can be used to estimate fault slip rates (e.g. Khajavi et al., 2018). Despite considered efforts, many earthquakes occur on previously unmapped faults (Quigley et al., 2010) and many active fault databases are recognised as incomplete (Nicol et al., 2016). To better characterise fault-based seismic hazard analysis, detailed mapping of evidence for surface rupturing earthquakes is required.

Mapping of neotectonic features from remotely sensed elevation and imagery data is commonly the first stage of creating a fault database as it allows identification of potential faults

over a large area. Faults may also be mapped in existing geological maps, and offsets of geological units can be interpreted in conjunction with remotely sensed data to gain an understanding of a fault's long-term activity rate. Remote mapping also provides a foundation to identify locations for subsequent fieldwork to more accurately characterise fault kinematics, slip rate and timing of past ruptures.

Australia has lower seismic hazard (Allen et al., 2020, 2023) than plate boundary settings (e.g. Western USA, Field et al., 2014; New Zealand, Gerstenberger et al., 2024; Indonesia, Irsyam et al., 2017) but has a rich historical record of ground surface rupturing earthquakes (King et al., 2018). A generally east-west compressive crustal stress regime has been in place in Southeastern Australia since the Late Miocene (5-10 Ma) (Rajabi et al., 2017), marking the "Neotectonic Era" (Clark et al., 2012). Neotectonic features are faults which have "hosted displacement under conditions imposed by the current Australian stress regime, and hence may move again in the future' (Clark, 2010; Clark et al., 2012). The Australian Neotectonic Features Database (ANFD) contains over 400 mapped neotectonic features, which are used to develop the fault source model in the Australian National Seismic Hazard Assessment (Allen et al., 2020, 2023; Clark et al., 2016)

The Snowy Monaro region forms the most elevated part of the southeastern highlands of Australia (Figure 1). While it has been debated how much of the present elevation of the highlands is relict, there is considerable evidence for Neogene relief generation in the form of stream derangements, displaced Cenozoic basalts and obvious fault scarps (Bishop, 1985; Clark et al., 2017; Irving & Green, 1976; Moye et al., 1963; Ollier, 1988; Sharp, 2004). A number of neotectonic features show evidence for late Cenozoic and Quaternary activity in the form of faulted fluvial deposits, youthful range front morphology and impoundment of rivers (Clark et al., 2017). Recent paleoseismic investigations have shown that the Jindabyne Thrust has evidence for Holocene rupture (Griffin et al., 2024).

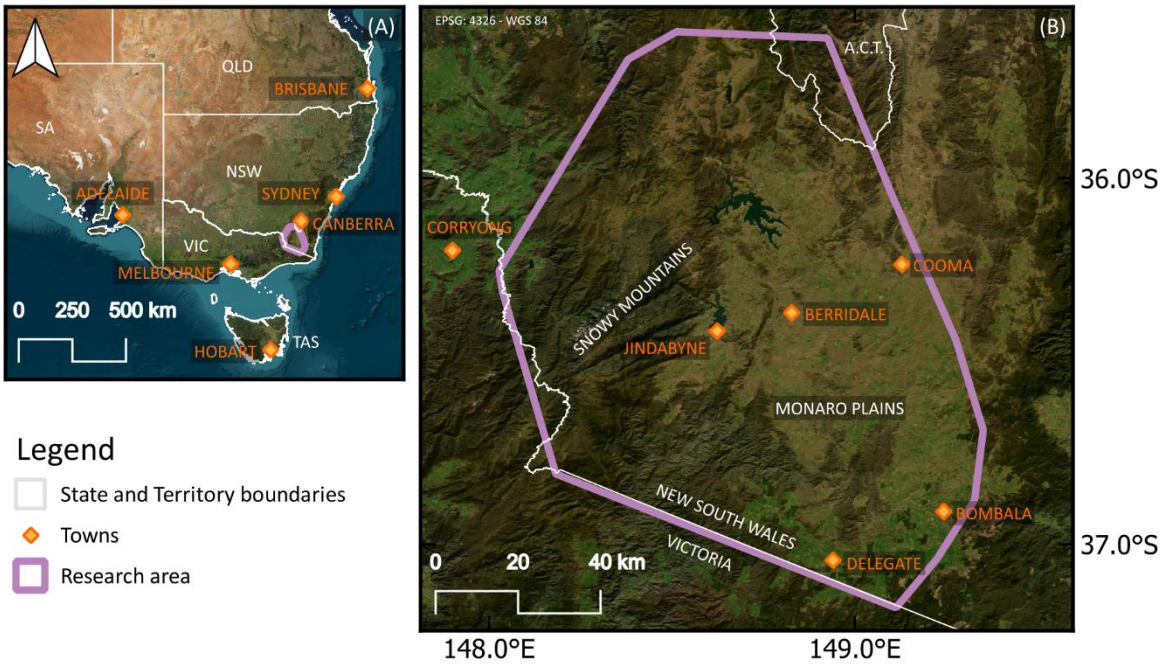

Figure 1: The research area is located between the Southern ACT border and the NSW/VIC state boundary (A) and encompasses the Snowy Mountains and Monaro Plains regions (B).

Prior to this research, it was only a very limited area of the Snowy Monaro region which had been mapped using high-resolution data (Griffin et al. 2024). Most other features recorded in the ANFD have geometries based on 1:100,000 and 1:250,000 geological map sheets, so lidar elevation data provides an opportunity to improve mapping resolution. Even so, the identification and analysis of neotectonic features in the region is challenging; extensive vegetation obscures satellite imagery, localised last-glacial glaciation solifluction and jointed

bedrock can be mistaken for fault trace lineaments, and erosion rates exceed slip rates, removing evidence of rupture (Clark et al., 2017; Heimsath et al., 2000, 2001, 2010). Here we undertake fault trace mapping and analysis of near-fault geomorphic features to update the neotectonic features database for the Snowy Monaro region. We assign confidence rankings to mapped features and use scaling relationships to estimate their potential maximum magnitudes. The results are relevant to future seismic hazard analyses and infrastructure exposure analyses in this region.

2 Methodology

2.1 Data used

Topographic mapping was conducted using a 2 m resolution lidar digital elevation model (DEM) mosaic from NSW Government Spatial Services (Figure 2). The lidar was acquired between 2017 and 2018, with 0.3 m vertical and 0.8 m horizontal accuracies (at 95% confidence). The availability of this high spatial resolution data is what prompted and enabled this research.

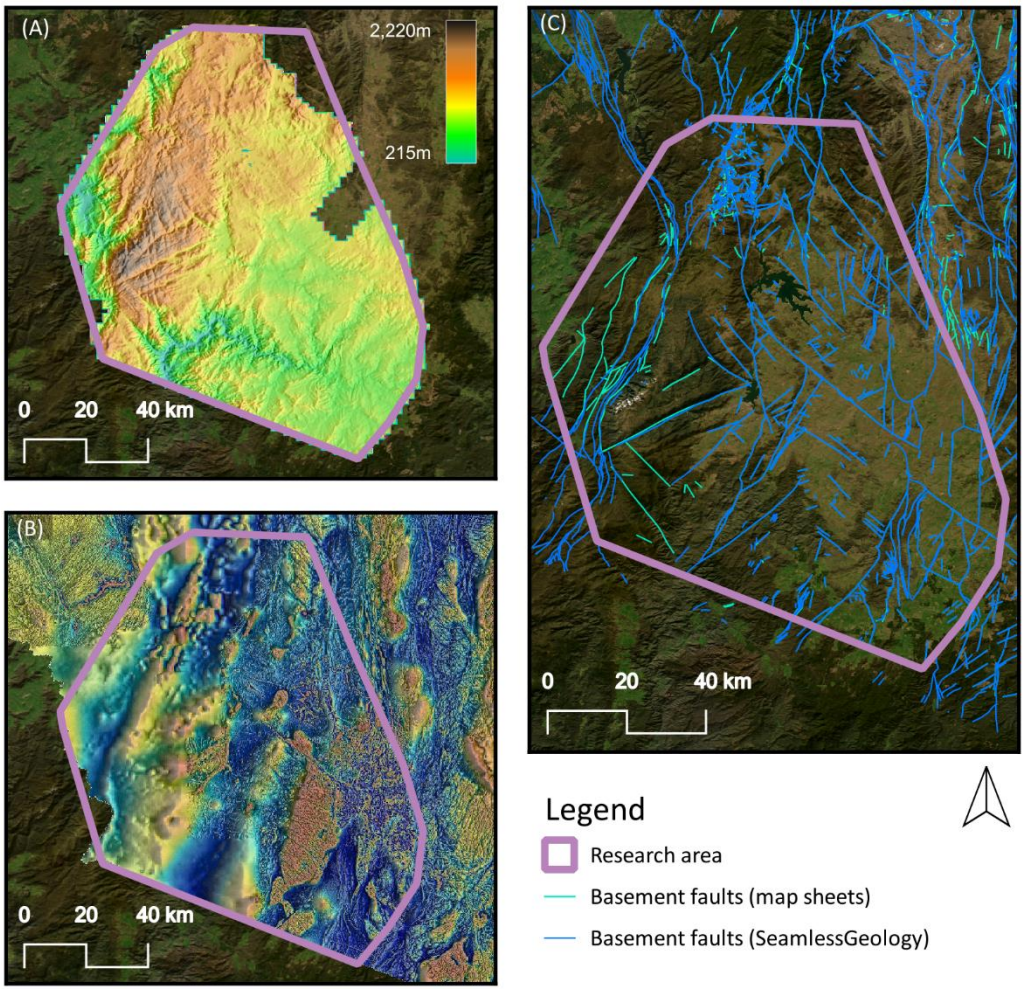

Figure 2: The three primary data sources used to inform the remote mapping process; lidar DEM with colour mapping (A), Total Magnetic Intensity (TMI) imagery (B), and basement fault datasets (C).

The NSW Government's SeamlessGeology dataset and 1:250,000 geological map sheets (Booker, 1965; Degeling, 1980; Lewis et al., 1994; Strusz, 1971) were used to inform the identification of basement faults, geological fabrics, and stratigraphic/erosional contacts (Figure 2). While the geological map sheets are misaligned with the SeamlessGeology dataset in places, the general positioning is similar between the two datasets, so is unlikely to have

impacted this research significantly. Where required, the mapping provided by SeamlessGeology is given preference due to its more recent collation.

Total Magnetic Intensity (TMI) data (Figure 2B) is also used to identify boundaries between geologic bodies in the subsurface and representations of magnetic structures which can be evidence of fault movement.

2.2 Revising existing mapping

Previously mapped ANFD features were investigated by identifying geomorphic evidence of past coseismic surface displacements along the existing mapped trace's strike. Where topographic evidence was found that suggested a deviation from the original mapped trace, the line was redrawn to reflect it. If no evidence was identified, the existing linework was carried over to ensure that the whole fault was represented by the trace mapping with no large gaps that would suggest a discontinuous fault geometry. A series of revisions were made to all stages of the linework.

2.3 Identifying new features

There is currently no standardised process for remotely identifying neotectonic features in Australia, so we adapt the method of Scott et al. (2023) and apply it to fault mapping of the Snowy Monaro region. We use a muti-stage, broad-to-detailed mapping process (see below) to identify five previously unmapped features in the research area. These features are estimated to have the potential to host earthquakes of up to M_W 7.0 based on mapped fault length, explained in Section 2.4. Based on the neotectonic evidence identified, the newly mapped features are classified with the same confidence ratings used in the Australian Neotectonic Features Database; *A* (Definite neotectonic feature), *B* (Probable neotectonic feature), *C* (Possible neotectonic feature) and *D* (Unlikely to be a neotectonic feature). Modelling fault rupture scenarios and conducting field research are outside the scope of this paper, but they are identified as the next steps in analysing fault hazard. New features identified in this study were named based on local geographic features and in consultation with Monaro/Snowy Mountains Traditional Custodians, who provided naming suggestions derived from place names in the local language.

Lineament mapping

We conducted manual mapping of DEM and TMI datasets to produce regional-scale lineament maps. Topographic lineament mapping highlights the extensive arrays of linear, structurally controlled valleys and ridgelines in the region. Models and algorithms to automate the edge-detection process for magnetic datasets (Bournas et al., 2003; Jacques et al., 2014; Yan et al., 2019) have not been used here but provide opportunities for future research. Areas which show overlap of topographic and geophysical lineaments and no indication of previously-mapped faults are identified as areas of interest for further investigation using the Geomorphic Indicator Ranking system (below).

Geomorphic Indicator Ranking system

The mapping of previously unmapped faults relies on the identification of geologic and / or topographic evidence for past, surface-rupturing earthquakes. Scott et al. (2023) created a system to standardise remote mapping of neotectonic faults based on the identification of geomorphic evidence of faulting. This approach fundamentally relies on the assumption that these features are preserved in the landscape (Scott et al., 2023). We rework their Geomorphic Indicator Ranking (GIR) system to better suit the tectonic and geomorphic context of the Snowy Monaro region, where there is significantly less seismicity and higher erosion rates than the locations featured in Scott et al.'s (2023) research. In their GIR system, they assigned values to each type of evidence (scarps, offset alluvial fans, linear valleys, etc.) to reflect the likelihood that the observed geomorphic feature was produced by, or associated with, neotectonic faulting. They used those values to compute the most likely location of a trace, however in our implementation we use qualitative DEM mapping to identify trace locations using the

indicators. Here, various features (e.g. linear rivers, bedrock scarps, knickpoints, and stream sinuosity changes) were identified and classified based on the GIR system and used to inform the classification of each newly mapped fault (using the NFD's confidence ratings). We approach the progression from mapped indicators to mapped fault traces in a more subjective way than Scott et al. (2023), relying on multiple revisions and reviews of the traces by the authors of this paper.

Profiling

Topographic profiling was conducted on fluvial terraces to determine the minimum offset of young (presumed Quaternary) sediments and fault geometry. Swath profiles were used, which returned mean, maximum and minimum elevation values relating to the distance along a central profile line within an area 10 m either side of the central line. Profiling an area rather than a line removes many errors caused by minor inaccuracies in the location of the profile, along with local topographic variations, which is especially useful in regions of complex geomorphology.

2.4 Maximum magnitude estimation

The potential maximum magnitude for each fault is calculated using a weighted average of 4 scaling relationships; Yang (Yang et al., 2021), Somerville (Somerville, 2021), Leonard, and Leonard (incorporating area) (Leonard, 2014). Maximum potential magnitudes are calculated using two different length measurements; preferred length (which refers to the length of observable surface rupture traces), and maximum length (the maximum probable length based on geophysical boundaries/lineaments). Leonard (2014) notes that faults which have surface ruptures longer than 50 km are likely to be down-dip width limited (Leonard, 2014) (i.e. the fault area is constrained by the seismogenic depth). For these faults, scaling relationships which incorporate fault area are more appropriate for estimating maximum potential magnitudes. We have assigned greater weighting values to area-based scaling relationships in our estimates as 52% of mapped faults in the research area show surface ruptures that are longer than 50 km.

Clark et al. (2012) classified Australia into seven neotectonic domains. The Snowy Monaro Region is within the Phanerozoic Accretionary Crust, for which the seismogenic depth is assumed to be 20 km. We use this value in Leonard (area) and Somerville Mw estimations for the down-dip fault width value. We assume fault dips of 30 degrees for reverse faults and 90 degrees for strike-slip faults, based on Andersonian theory (Anderson, 1905), for maximum magnitude calculations, but note that in most situations we have no real constraint on fault dip.

Table 1: Weighting for Mw estimates.

Scaling relationship	Input variable	Weighting
Yang	Length	0.1
Leonard	Length	0.2
Somerville	Area	0.35
Leonard	Area	0.35

There are inherent assumptions associated with each scaling relationship and their application in this study. Future studies will investigate the faults individually to gain deeper insights into rupture behaviours, producing more reliable Mw potential estimates.

3 Results

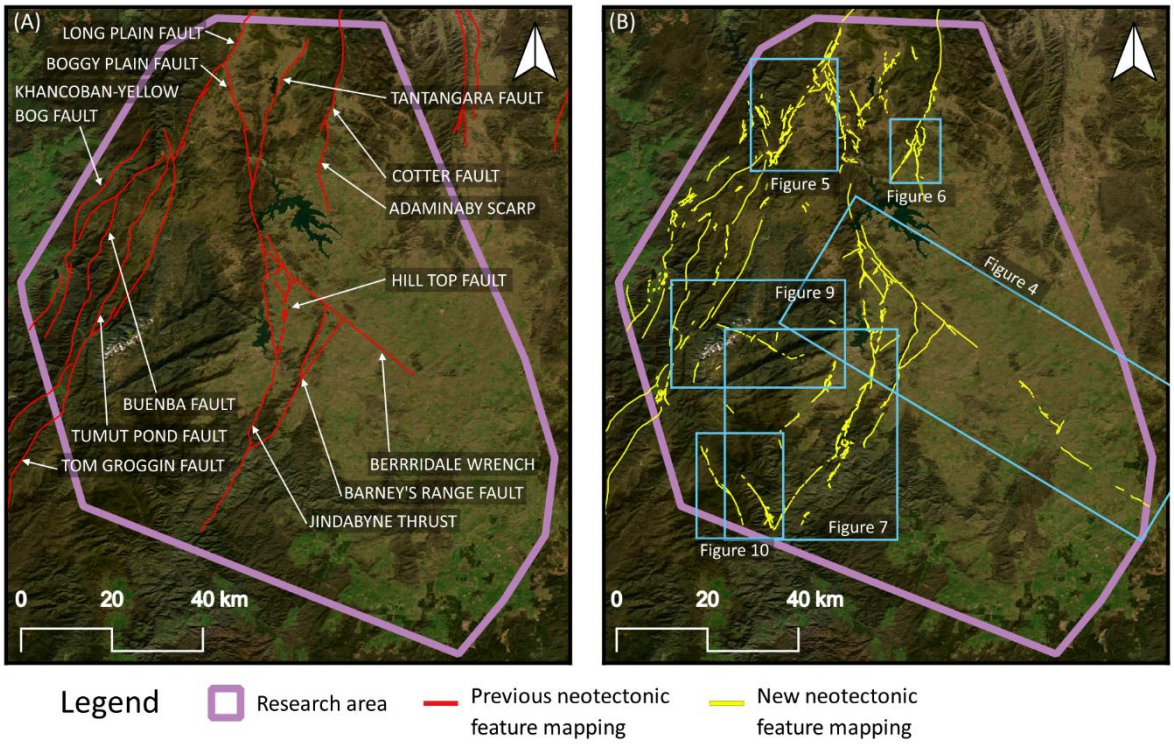

Figure 3: Neotectonic feature mapping; current ANFD lines (A) and new lines (B).

3.1 Existing features

The revisions to the existing NFD traces are varied, as some fault traces remain the same and some are significantly revised in their locations and extents. The most noteworthy changes to existing features are detailed below.

Adaminaby Scarp and Cotter Fault Zone (ACFZ)

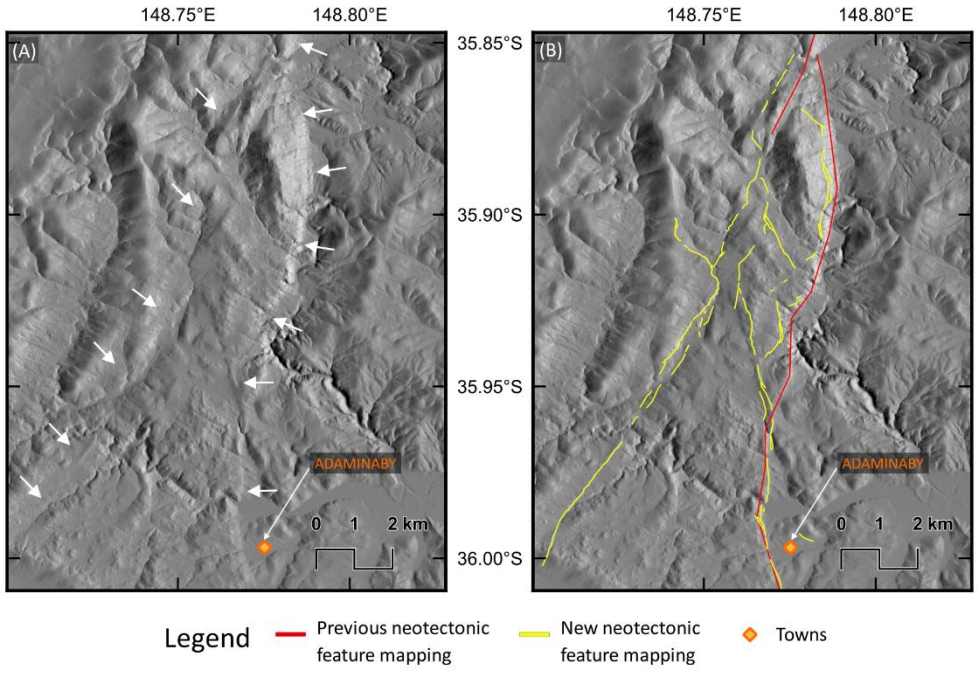

Figure 4: Adaminaby Scarp and Cotter Fault Zone shown uninterpreted (A) and interpreted (B).

The Adaminaby Scarp and Cotter Fault Zone (ACFZ), between Adaminaby town and the NSW-ACT border, includes two faults previously identified as discrete to each other. Evidence supporting their identification as a fault zone includes similarities in the strikes and geometries of the two faults, and the complex rupture traces between them (Figure 4). Surface ruptures associated with Cotter Fault have been identified extending 15 km southwest of the existing mapped traces, truncated by a basement fault with a perpendicular strike (Figure 4).

Berridale Fault

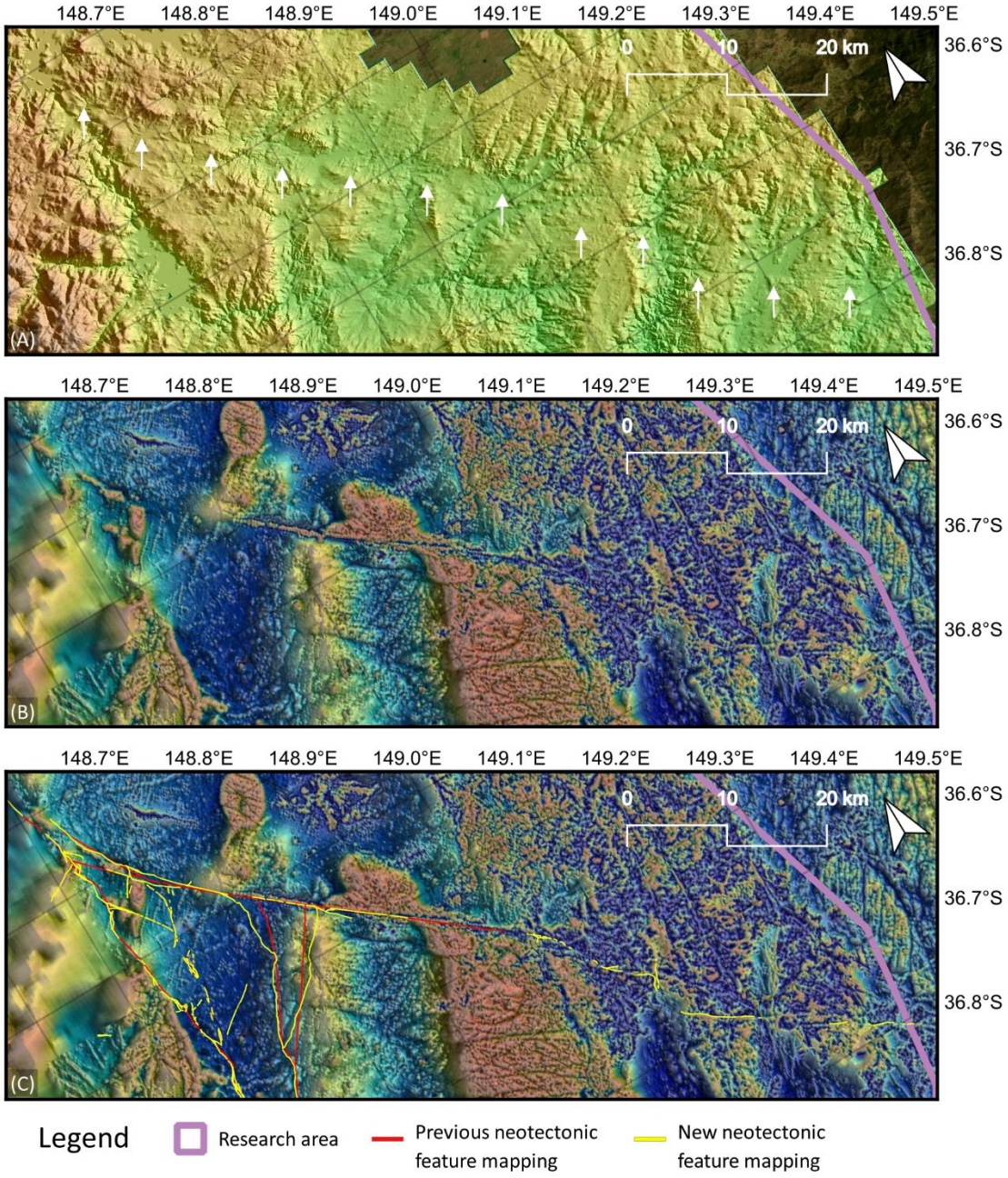

Figure 5. The Berridale Fault, shown on uninterpreted lidar DEM (A) and magnetic (B) maps, and interpreted on the magnetic map (C). Note that the view has been rotated, refer to Figure 3 for context. White arrows indicate the location of the mapped fault traces.

Traces of the Berridale Fault are identified 52 km farther southeast than the existing mapped trace, almost doubling the mapped length of the fault. These traces show less vertical offset than in the northwest of the fault, but they follow magnetic and topographic lineaments that suggest continuity (Figure 5).

Long Plain Fault

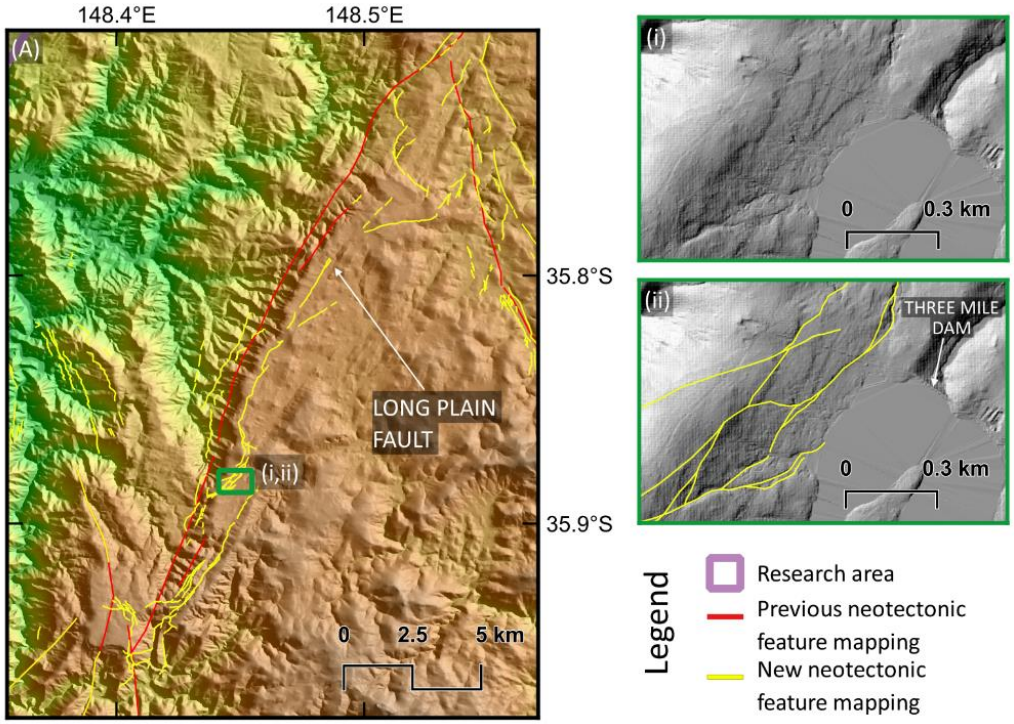

Figure 6: Long Plain Fault traces (A), shown uninterpreted (i) and interpreted (ii).

We mapped lineaments near Three Mile Dam (Figure 6), 1 km closer to the dam than previous mapping. Based on their surface-rupture-like pattern, these lineaments are potential evidence of neotectonic surface rupture.

3.2 Newly identified features

Moyungal Fault

The Moyungal Fault is identified as a northeast striking fault, located parallel to the southern end of the Jindabyne Thrust. The fault is characterised by sharp bedrock scarps which are exposed on hillslopes (Figure 7Ai, 6Bi) and absent in gulleys, however, evidence persists in geomorphic indicators (mainly stream diversions) which align with the fault's strike. Along the fault, scarps show vertical offset both sides of the fault trace, suggesting that it may have strike-slip geometry, an interpretation supported by its apparent subvertical dip. Geomorphic evidence of faulting extends for 34 km along strike and aligns with a bedrock structure at its southern end (Figure 7). Vertical offset is interpreted as a minimum of 0.9 m based on swath profiling of young (presumed Quaternary) sediments along a fluvial terrace (Figure 8) This is the strongest direct evidence of neotectonism for any of this paper's newly identified features. The sharp morphology of the hillslope scarps supports this as secondary evidence of neotectonic movement. The fault has been assigned a confidence rating of B – probable neotectonic feature, the highest rating that can be assigned without supporting field analysis.

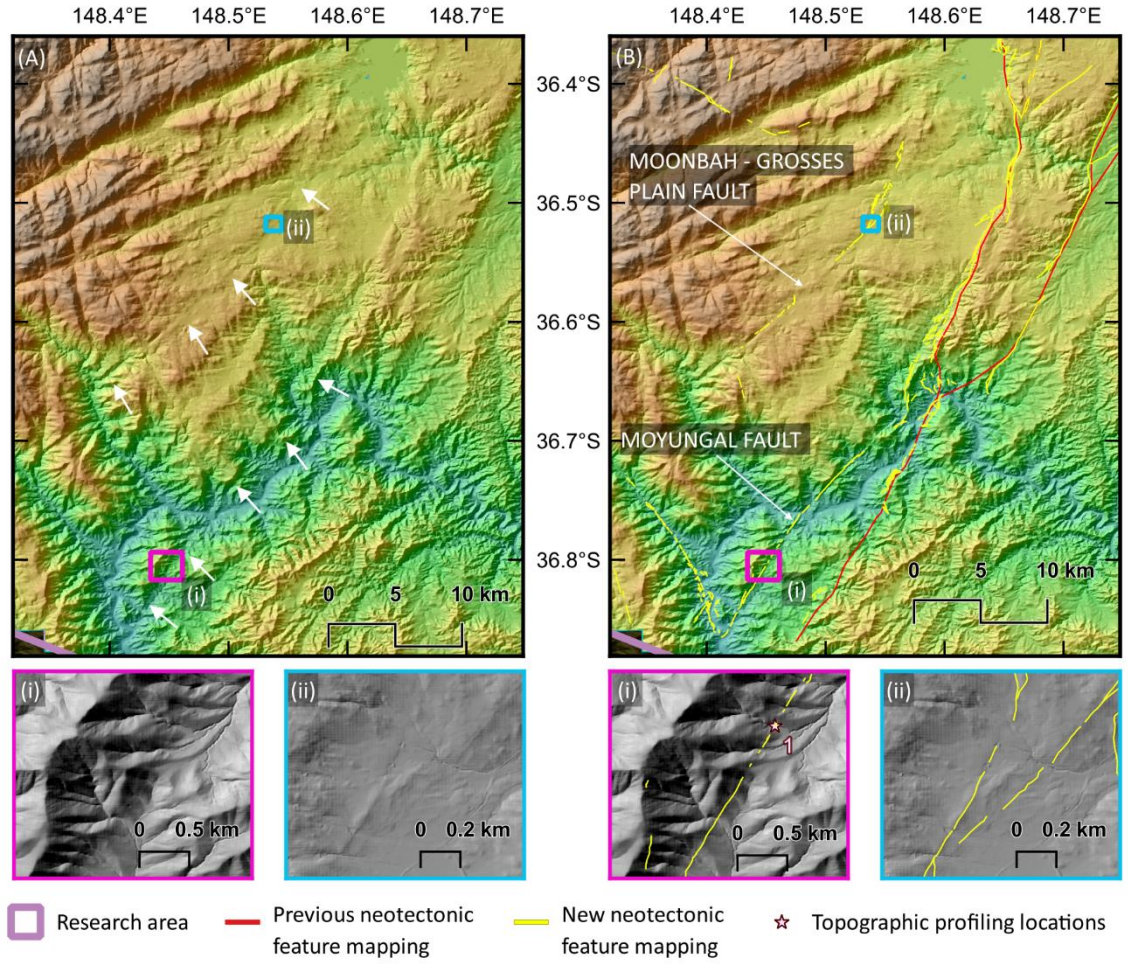

Figure 7: Moyungal (A, i – pink inset) and Moonbah - Grosses Plain (ii – blue inset) Faults shown uninterpreted (A) and interpreted (B) on lidar DEM. Insets (Ai, Aii, Bi, Bii) show details of the fault traces. White arrows indicate the location of the mapped fault traces.

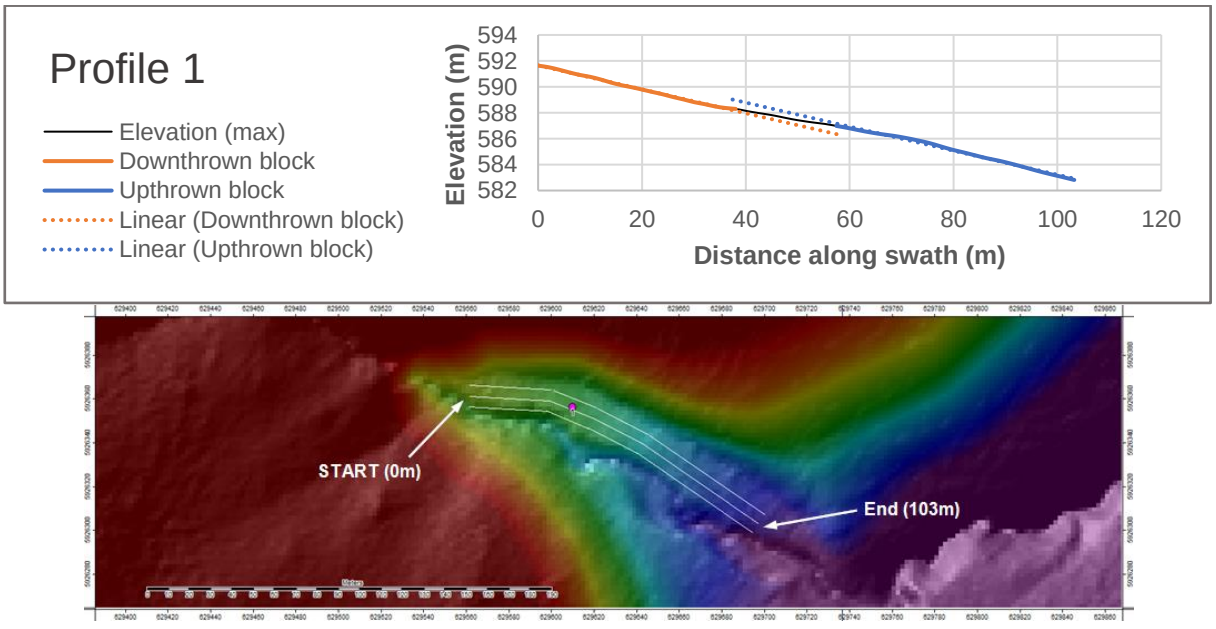

Figure 8: Topographic swath profile (top) and location along terrace (bottom), where high-low (red-blue) elevation colour mapping was applied to the DEM. Point 1 (pink circle) refers to Swath Profile Location 1 in Figure 7Bi.

Moonbah - Grosses Plain Fault

Located 20 km north of (and parallel to) the Moyungal Fault, the Moonbah – Grosses Plain Fault is observed to splay into two traces at its northern end (Figure 7). The main trace is 15 km long, and the splays are 9 km and 3 km long, striking north and northeast respectively. The geometry of the fault is unknown, but Lewis et al. (1994) briefly mention that the underlying basement fault (Grosses Plain Fault) shows right-lateral displacement, so we have described it as strike-slip for our magnitude estimations (Table 2). Many of the features that could indicate neotectonic offset are obstructed or altered anthropogenically (e.g. via the damming of streams), and the unaltered features do not show any measurable offset. The fault has therefore been assigned a confidence rating of C – possible neotectonic feature, as there is inadequate evidence to disprove the occurrence of a neotectonic rupture but similarly not any direct evidence to support it.

Perisher Fault

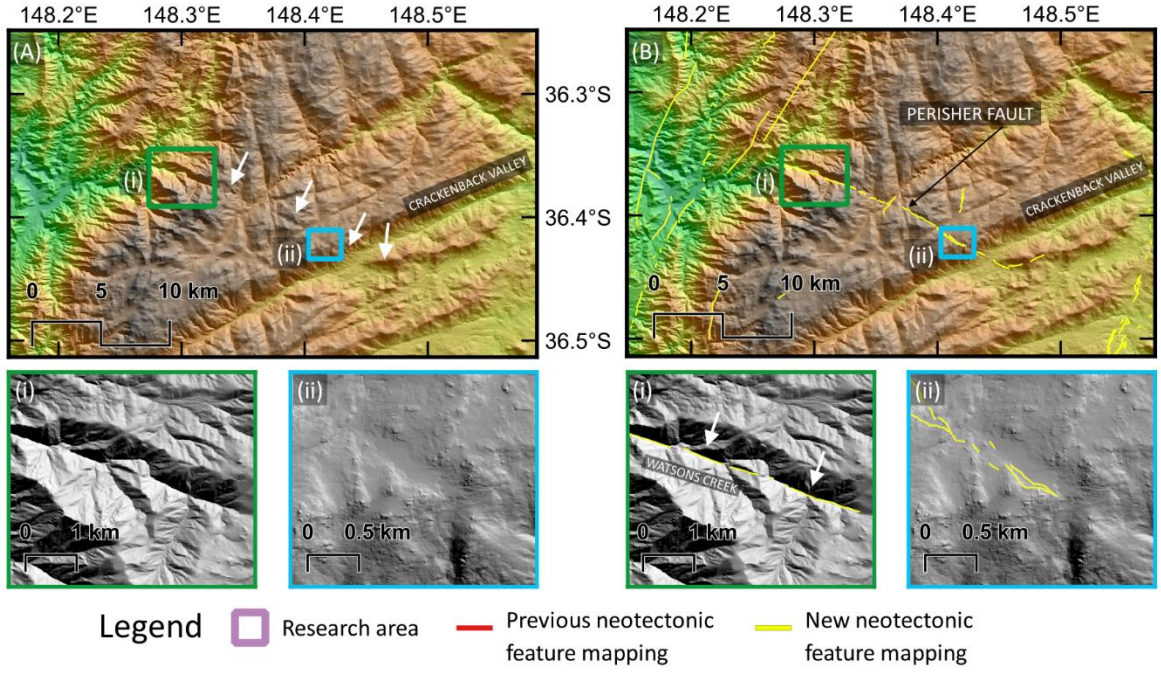

Figure 9: Perisher Fault shown uninterpreted (A) and interpreted (B) on lidar DEM. Insets (Ai, Aii, Bi, Bii) show details of the fault traces. White arrows indicate the location of the mapped fault traces.

Possible surface traces of the Perisher Fault have been identified over a length of 22 km. These were initially identified from two linear segments of Watson's Creek at its northern end (Figure 9Ai, 8Bi). Minor evidence for the fault continues farther southeast across the Kosciuszko Block (plateau), in the form of stream diversions and topographic lineaments (Figure 9Aii, 8Bii), with some evidence identified south of the Crackenback Valley. The geometry of this fault has not been determined at this stage of research, but for the purposes of magnitude estimates it has been tentatively interpreted as a thrust fault, based on the vertical offset of lineaments. The Perisher Fault strikes parallel to the current compressive stress regime of the region (Rajabi et al., 2017), so neotectonic offset is unlikely unless the fault has been affected by local stress field changes related to other faults in the region. Though there is a lack of evidence to suggest that it has moved under the current stress regime, the feature may indeed be tectonically produced. For the ANFD, it has been assigned the confidence rating of D – Unlikely to be a neotectonic feature.

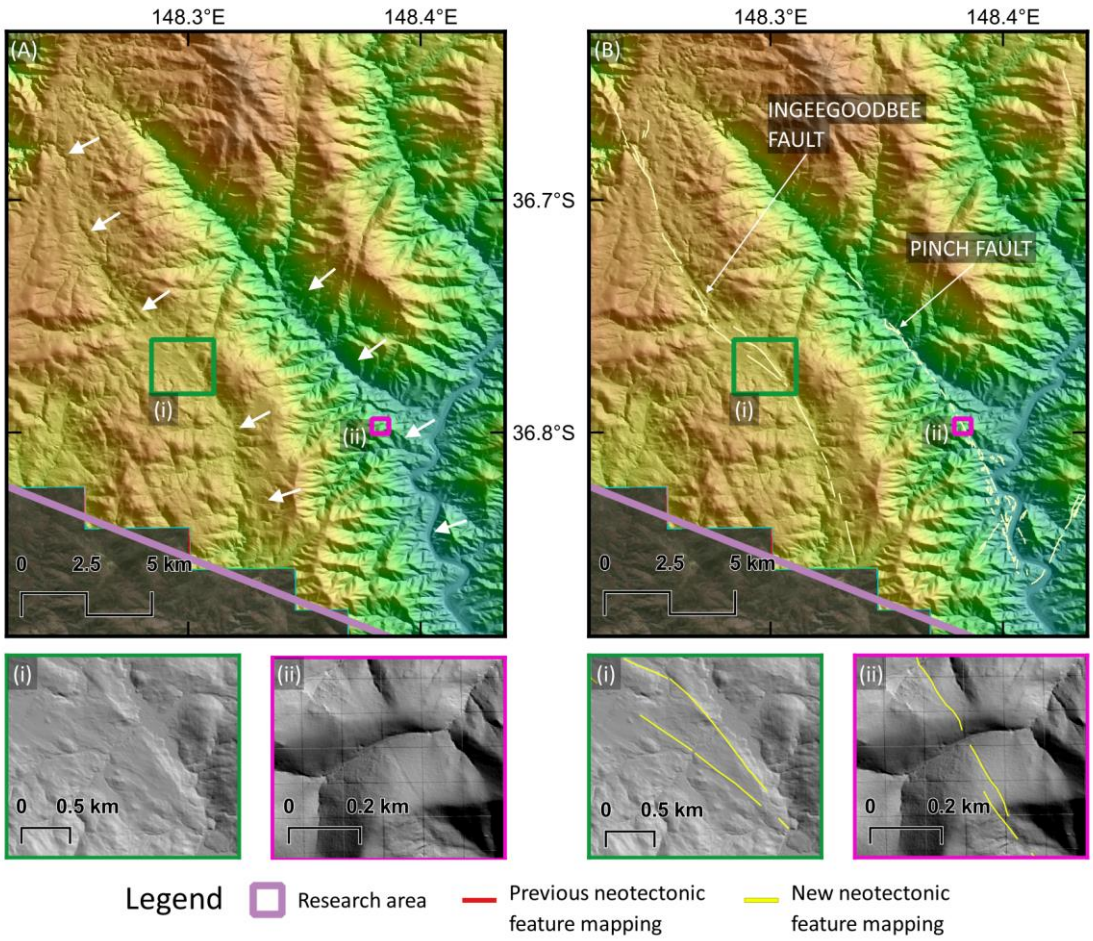

Figure 10: Ingeegoodbee (i – green inset) and Pinch (ii – blue inset) Faults shown uninterpreted (A) and interpreted (B) on lidar DEM. Insets (Ai, Aii, Bi, Bii) show details of the fault traces. Orange arrows indicate the location of the mapped fault traces.

Pinch Fault

The Pinch Fault is located in a northwest-southeast oriented linear valley aligned with the Pinch River (Figure 10). Observed traces of the fault extend for 15 km, with complex rupture patterns located at its southern end where it may interact with the Moyangul Fault. An existing basement fault was identified by Booker (1965) which may be the feature that results in the valley's linear morphology. In a rupture event, the length of the fault may have the potential to propagate a further 19 km if the rupture propagated along the basement fault. In the southeastern end of the valley, sharp scarps were identified as potential neotectonic evidence but may be associated with deeply jointed bedrock rather than faulting. Swath profiling was conducted along fluvial terraces and no measurable vertical offset was found. This fault has been assigned the confidence rating of D - Unlikely to be a neotectonic feature.

Ingeegoodbee Fault

This fault is located in a northwest-southeast oriented linear valley drained by the Ingeegoodbee River, where there is no basement fault previously identified. The fault follows the river valley and is characterised by scarps along its banks (Figure 10Ai, 9Bi). Geomorphic evidence of faulting is mapped for 24 km along strike. This fault has been assigned the confidence rating of C - Possible neotectonic feature.

3.3 Maximum magnitude estimates

Fault lengths, areas, and weighted Mw estimates are presented in Table 2. It should be noted that these magnitude estimates are derived from scaling relationships, and seismogenic depths and fault dips are assumed, and therefore are subject to considerable uncertainties.

Table 2: Potential Mw estimations, Preferential (pref) and maximum (max) lengths are used to calculate the fault area and the estimation of maximum credible earthquake Mw.

	Fault name (SS = strike slip, RV = reverse faulting)	**Fault length** (pref, max) [km]		**Fault area** (pref, max) [km^2]		**Weighted Mw** (pref, max)	
New features	Moyungal Fault SS	34	41	684	821	7.0	7.1
	Moonbah - Grosses Plain Fault SS	15	40	294	793	6.6	7.0
	Perisher Fault RV	22	25	872	983	7.0	7.0
	Pinch Fault RV	14	32	540	1,287	6.7	7.1
	Ingeegoodbee Fault RV	24	24	947	974	7.0	7.0
Previously mapped features	Khancoban - Yellow Bog Fault RV	62	81	2,488	3,254	7.5	7.7
	Buenba Fault RV	107	119	4,284	4,778	7.8	7.9
	Tumut Pond Fault RV	67	70	2,688	2,793	7.6	7.6
	Tom Groggin Fault RV	109	117	4,372	4,669	7.8	7.9
	Long Plain Fault RV	97	99	3,897	3,961	7.8	7.8
	Boggy Plain Fault RV	31	34	1,248	1,343	7.2	7.2
	Tatangara Fault RV	29	42	1,164	1,683	7.1	7.3
	Adaminaby Cotter Fault Zone RV	70	112	2,800	4,468	7.6	7.8
	Jindabyne Thrust RV	85	107	3,408	4,273	7.7	7.8
	Hill Top Fault SS	24	25	480	508	6.8	6.8
	Barneys Range Fault RV	45	63	1,800	2,539	7.4	7.5
	Berridale Fault RV	104	138	4,140	5,511	7.8	7.9

4 Discussion and future research

The results presented here demonstrate the potential for the use of high resolution lidar data combined with geologic and geophysical data to improve understanding of the spatial extent and structural properties of neotectonic features in southeastern Australia. Through interrogation of new high lidar elevation data freely provided by the NSW Government we have been able to identify five previously unknown neotectonic features, in addition to constraining the location of previously known features. This represents a significant advance on previous

knowledge, where there is potential for similar studies to be undertaken in other parts of the southeastern highlands of Australia, and elsewhere around the country, using such elevation datasets.

Our research provides the foundation for future field investigations on faults in the Snowy Monaro region, and also provides a guide for future remote mapping of neotectonic features in Australia. Our adapted GIR system aims to begin a standardised remote mapping method, which is important for better understanding the locations and extent of fault-source seismic hazard.

While we describe our mapping as evidence of neotectonic features, it is quite obviously restricted to representing only earthquakes of sufficient displacement and Mw to cause ground surface rupture (e.g., >50% probability at Mw >6.0-6.2; Yang et al. 2021). No surface rupturing earthquakes have been observed in eastern Australia since European settlement, and significant events such as the 2021 M_W 5.9 Woods Point earthquake did not rupture the ground surface (Quigley and La Greca, 2021).

Future research is expected based on the results of this study. This will incorporate more detailed analysis of fault geometries, kinematics, field excavations, assessments of whether ruptures are segmented, and magnitude estimations for segmented and multi-fault ruptures.

5 References

Allen, T. I., Griffin, J. D., Clark, D. J., Cummins, P. R., Ghasemi, H., & Ebrahimi, R. (2023). *The 2023 National Seismic Hazard Assessment for Australia*. Geoscience Australia Record.

Allen, T. I., Griffin, J. D., Leonard, M., Clark, D. J., & Ghasemi, H. (2020). The 2018 national seismic hazard assessment of Australia: Quantifying hazard changes and model uncertainties. *Earthquake Spectra*, *36*(1_suppl), 5–43.

Anderson, E. M. (1905). The dynamics of faulting. *Transactions of the Edinburgh Geological Society*, *8*(3), 387–402.

Bishop, P. (1985). Southeast Australian late Mesozoic and Cenozoic denudation rates: A test for late Tertiary increases in continental denudation. *Geology*, *13*(7), 479–482. https://doi.org/10.1130/0091-7613(1985)13<479:SALMAC>2.0.CO;2

Booker, F. W. (1965). *Explanatory Notes: Tallangatta 1:250,000 Geological Series* (1st ed.). Department of Mines - Geological Survey of New South Wales.

Bournas, N., Galdeano, A., Hamoudi, M., & Baker, H. (2003). Interpretation of the aeromagnetic map of Eastern Hoggar (Algeria) using the Euler deconvolution, analytic signal and local wavenumber methods. *Journal of African Earth Sciences*, *37*(3), 191–205. https://doi.org/10.1016/j.jafrearsci.2002.12.001

Clark, D. (2010). Large earthquake recurrence in the Sprigg Orogen, South Australia and implications for earthquake hazard assessment. *Australian Geomechanics*, *45*, 41–52.

Clark, D., Leonard, M., Griffin, J., Stirling, M., & Volti, T. (2016, November). Incorporating fault sources into the Australian National Seismic Hazard Assessment (NSHA) 2018. *Australian Earthquake Engineering Society 2016 Conference*.

Clark, D., McPherson, A., Pillans, B., White, D., & MacFarlane, D. (2017). *Potential geologic sources of seismic hazard in Australia's south-eastern highlands: What do we know?* Australian Earthquake Engineering Society Conference, Canberra, ACT.

Clark, D., McPherson, A., & Van Dissen, R. (2012). Long-term behaviour of Australian stable continental region (SCR) faults. *Tectonophysics*, *566–567*, 1–30. https://doi.org/10.1016/j.tecto.2012.07.004

Degeling, P. R. (1980). *Explanatory Notes: Wagga Wagga 1:250 000 Metallogenic Series*. Geological Survey of New South Wales.

Field, E. H., Arrowsmith, R. J., Biasi, G. P., Bird, P., Dawson, T. E., Felzer, K. R., Jackson, D. D., Johnson, K. M., Jordan, T. H., Madden, C., Michael, A. J., Milner, K. R., Page, M. T., Parsons, T., Powers, P. M., Shaw, B. E., Thatcher, W. R., Weldon, R. J., II, & Zeng, Y. (2014). Uniform California Earthquake Rupture Forecast, Version 3 (UCERF3)—The Time-Independent Model. *Bulletin of the Seismological Society of America*, *104*(3), 1122–1180. https://doi.org/10.1785/0120130164

Gerstenberger, M. C., Van Dissen, R., Rollins, C., DiCaprio, C., Thingbaijim, K. K. S., Bora, S., Chamberlain, C., Christophersen, A., Coffey, G. L., Ellis, S. M., Iturrieta, P., Johnson, K. M., Litchfield, N. J., Nicol, A., Milner, K. R., Rastin, S. J., Rhoades, D., Seebeck, H., Shaw, B. E., … Williams, C. (2024). The Seismicity Rate Model for the 2022 Aotearoa New Zealand National Seismic Hazard Model. *Bulletin of the Seismological Society of America*, *114*(1), 182–216. https://doi.org/10.1785/0120230165

Griffin, J., Clark, D., Kemp, J., Stirling, M., King, T., Kulesza, O., Greca, J., Sharma, A., Quigley, M., Ninis, D., Pietsch, T., Eaton, B., & Wilcken, K. (2024). Large earthquake recurrence in the Snowy Monaro region: New findings to inform dam safety. *Proceedings of the 2024 ANCOLD Conference*.

Heimsath, A. M., Chappell, B. W., & Fifield, K. (2010). Eroding Australia: Rates and processes from Bega Valley to Arnhem Land. *Geological Society of London Special Publication*, *346*, 225–242.

Heimsath, A. M., Chappell, J., Dietrich, W. E., Nishiizumi, K., & Finkel, R. C. (2000). Soil production on a retreating escarpment in southeastern Australia. *Geology*, *28*(9), 787–790. https://doi.org/10.1130/0091-7613(2000)28<787:SPOARE>2.0.CO;2

Heimsath, A. M., Chappell, J., Dietrich, W. E., Nishiizumi, K., & Finkel, R. C. (2001). Late Quaternary erosion in southeastern Australia: A field example using cosmogenic nuclides. *Quaternary International*, *83–85*, 169–185. https://doi.org/10.1016/S1040-6182(01)00038-6

Irsyam, M., Asrurifak, M., Mikhail, R., Wahdiny, I. I., Rustiani, S., & Munirwansyah, M. (2017). Development of Nationwide Vs30 Map and Calibrated Conversion Table for Indonesia using Automated Topographical Classification. *Journal of Engineering and Technological Sciences*, *49*(4), 457–471. https://doi.org/10.5614/j.eng.technol.sci.2017.49.4.3

Irving, A. J., & Green, D. H. (1976). Geochemistry and petrogenesis of the newer basalts of Victoria and South Australia. *Journal of the Geological Society of Australia*, *23*(1), 45–66. https://doi.org/10.1080/00167617608728920

Jacques, P. D., Machado, R., Oliveira, R. G. de, Ferreira, F. J. F., Castro, L. G. de, & Nummer, A. R. (2014). *Correlation of lineaments (magnetic and topographic) and Phanerozoic brittle structures with Precambrian shear zones from the basement of the Paraná Basin, Santa Catarina State, Brazil*.

Khajavi, N., Nicol, A., Quigley, M. C., & Langridge, R. M. (2018). Temporal slip-rate stability and variations on the Hope Fault, New Zealand, during the late Quaternary. *Tectonophysics*, *738*, 112–123.

King, T. R., Quigley, M. C., & Clark, D. (2018). Earthquake environmental effects produced by the Mw 6.1, 20th May 2016 Petermann earthquake, Australia. *Tectonophysics*, *747–748*, 357–372. https://doi.org/10.1016/j.tecto.2018.10.010

Leonard, M. (2014). Self-Consistent Earthquake Fault-Scaling Relations: Update and Extension to Stable Continental Strike-Slip Faults. *Bull. Seism. Soc. Am*, *104*, 2953–2965. https://doi.org/10.1785/0120140087

Lewis, P. C., Glen, R. A., Pratt, G. W., & Clarke, I. (1994). *Explanatory Notes: Bega-Mallacoota 1:250 000 Geological Series*. Geological Survey of New South Wales.

Moye, D. G., Sharp, K. R., & Stapledon, D. H. (1963). *Geology of the Snowy Mountains Region*. Snowy Mountains Hydro-Electric Authority.

Nicol, A., Van Dissen, R. J., Stirling, M. W., & Gerstenberger, M. C. (2016). Completeness of the Paleoseismic Active-Fault Record in New Zealand. *Seismological Research Letters*, *87*(6), 1299–1310. https://doi.org/10.1785/0220160088

Ollier, C. D. (1988). Deep Weathering, Groundwater and Climate. *Geografiska Annaler: Series A, Physical Geography*, *70*(4), 285–290. https://doi.org/10.1080/04353676.1988.11880258

Quigley, M., Villamor, P., Furlong, K., Beavan, J., Van Dissen, R., Litchfield, N., Stahl, T., Duffy, B., Bilderback, E., Noble, D., Barrell, D., Jongens, R., & Cox, S. (2010). Previously Unknown Fault Shakes New Zealand's South Island. *Eos, Transactions American Geophysical Union*, *91*(49), 469–470. https://doi.org/10.1029/2010EO490001

Rajabi, M., Tingay, M., Heidbach, O., Hillis, R., & Reynolds, S. (2017). The present-day stress field of Australia. *Earth-Science Reviews*, *168*, 165–189. https://doi.org/10.1016/j.earscirev.2017.04.003

Scott, C., Adam, R., Arrowsmith, R., Madugo, C., Powell, J., Ford, J., Gray, B., Koehler, R., Thompson, S., Sarmiento, A., Dawson, T., Kottke, A., Young, E., Williams, A., Kozaci, O., Oskin, M., Burgette, R., Streig, A., Seitz, G., … Ingersoll, S. (2023). Evaluating how well active fault mapping predicts earthquake surface-rupture locations. *Geosphere*, *19*(4), 1128–1156. https://doi.org/10.1130/GES02611.1

Sharp, K. R. (2004). Cenozoic volcanism, tectonism and stream derangement in the Snowy Mountains and northern Monaro of New South Wales. *Australian Journal of Earth Sciences*, *51*(1), 67–83.

Somerville, P. (2021). Scaling relations between seismic moment and rupture area of earthquakes in stable continental regions. *Earthquake Spectra*, *37*(1_suppl), 1534–1549.

Strusz, D. L. (1971). *Explanatory Notes: Canberra 1:250 000 Geological Series*. Department of National Development.

Wells, D. L., & Coppersmith, K. J. (1994). New empirical relationships among magnitude, rupture length, rupture width, rupture area, and surface displacement. *Bulletin of the Seismological Society of America*, *84*(4), 974–1002. https://doi.org/10.1785/BSSA0840040974

Yan, J., Chen, X., Meng, G., Lü, Q., Deng, Z., Qi, G., & Tang, H. (2019). Concealed faults and intrusions identification based on multiscale edge detection and 3D inversion of gravity and magnetic data: A case study in Qiongheba area, Xinjiang, Northwest China. *Interpretation*, *7*(2), T331–T345. https://doi.org/10.1190/INT-2018-0066.1

Yang, H., Quigley, M., & King, T. (2021). Surface slip distributions and geometric complexity of intraplate reverse-faulting earthquakes. *GSA Bulletin*, *133*(9–10), 1909–1929. https://doi.org/10.1130/B35809.1

Quigley, M., & La Greca, J. (2021). Reconnaissance survey of environmental and infrastructure damage from the September 2021 MW 5.9 Woods Point earthquake, Victoria, Australia. *Earthquake Engineering Research Institute—Australian Earthquake Engineering Society—New Zealand Society of Earthquake Engineering Joint Learning from Earthquakes Clearinghouse Woods Point, Australia Earthquake.*